ACS OMEGA

Open Access

This article is licensed under CC-BY-NC-ND 4.0

http://pubs.acs.org/journal/acsodf

Article

# Design of a Multi-Epitope Vaccine against the Glycoproteins of Newcastle Disease Virus by Using an Immunoinformatics Approach

Natolotriniavo T. Randriamamisolonirina,* Mirantsoa S. Razafindrafara, and Olivier F. Maminiaina

Cite This: *ACS Omega* 2025, 10, 4007−4018

Read Online

ACCESS | Metrics & More | Article Recommendations | Supporting Information

**ABSTRACT:** Newcastle disease (ND) causes major economic losses in poultry farming in Madagascar and many other countries. Previously, vaccines based on attenuated or inactivated Newcastle disease viruses (NDV) have been effective against this disease. However, their efficacy has declined due to viral mutations over time. To address this, two new multi-epitope vaccines (MEV) have been designed using immunoinformatics methods. First, 26 conserved epitopes from the fusion protein and 22 from the hemagglutinin-neuraminidase protein of 12 NDV strains isolated in Madagascar were selected to design the MEV. These epitopes were fused with specific linkers. Additionally, the adjuvant Avian Beta-Defensins-1 and the 6xHis tag were added to the N- and C-terminal ends of the vaccine formulations, respectively. The antigenicity, allergenicity, solubility, and physicochemical properties of the designed MEV were evaluated. Their three-dimensional structures were also modeled. Molecular docking studies and dynamic simulations were then conducted with the chicken Toll-like receptor 7 (TLR7) to assess the binding affinity of the MEV with this receptor. Finally, an immunological simulation was carried out to assess the ability of the candidate vaccine to induce an effective immune response. Through immunoinformatics analysis, both MEVs developed in this study were found to be highly antigenic, nonallergenic, and physicochemically stable. In addition, they showed significant interaction with the TLR7 receptor. They also have the capacity to trigger immune responses and promote the formation of memory cells following immunization. Therefore, these vaccines represent promising candidates for the control of ND. As this is an immunoinformatics study based on *in silico* methods, both *in vitro* and *in vivo* experiments are required to confirm and extend these results.

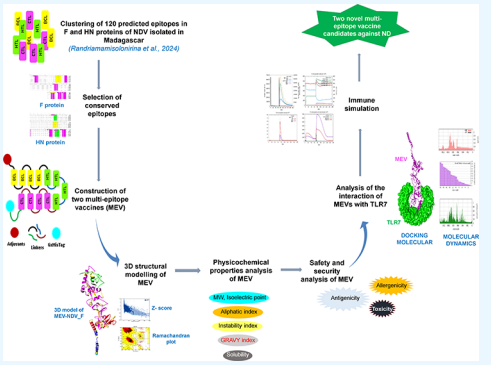


## 1. INTRODUCTION

Newcastle disease (ND) is a highly contagious disease affecting many species of domestic and wild birds. It is caused by the Newcastle disease virus (NDV), belonging to the genus *Avian orthoavulavirus-1* (AoAV-1), family Paramyxoviridae and order Mononegavirale. Currently, twenty-two (22) genotypes of AoAV-1 have been identified in various bird species.[1]

NDV are large, pleomorphic viruses with a single-stranded RNA genome of negative polarity.[2] This genome comprises six structural genes, encoding six structural proteins including phosphoprotein P, hemagglutinin-neuraminidase HN, nucleoprotein NP, large protein L, fusion protein F and matrix protein M.[3] Two accessory proteins V and W, are also produced by RNA editing during transcription of the P gene.[4]

The F and HN proteins are membrane glycoproteins. The HN protein is involved in the binding of the virus to the receptor of infected host cells, promoting fusion by interaction with glycoprotein F.[5] On the other hand, F protein is responsible for both the fusion and penetration of the virus into the host cell.[2] Consequently, both proteins represent important targets for the host immune response, and are essential for the development of effective ND vaccines.[6]

Vaccination remains the only means of preventing ND. Commercially available Newcastle vaccines are generally based on genotype I, II and III strains.[7] These vaccines have been shown to be effective in reducing morbidity and mortality in poultry.[8] However, their inability to prevent viral shedding against wild strains poses a major challenge to the control of ND in the long term. This failure is essentially due to the genetic distance between the wild strains circulating in poultry farms and the strains used for vaccine production.[9] Therefore, some studies have highlighted the importance of using vaccine strains derived from strains currently circulating in farms to minimize viral shedding.[10−12]

Recently, inactivated prototype vaccine was developed by our team,[13] using the MG-1992 strain isolated in Madagascar in 1992 and belonging to genotype XI.[14] Although this vaccine has proved encouraging in preventing clinical disease and outperforming the vaccine based on the Mukteswar strain, crucial aspects such as stability, safety, sterility and duration of

Received: October 30, 2024
Revised: December 24, 2024
Accepted: December 30, 2024
Published: January 22, 2025

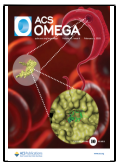

© 2025 The Authors. Published by American Chemical Society

Table 1. List of Conserved Epitopes in F and HN Proteins of NDV[a]

| protein | epitope group | epitope code | position | peptide | Score VaxiJen | allergenicity | membrane topology |
|---|---|---|---|---|---|---|---|
| protein F | epitope B | $E_1$ | 29−36 | TSSLDGRP | 1.3312 | NA | EM |
| | | $E_2$ | 222−232 | GPQITSPALTQ | 0.4337 | NA | EM |
| | | $E_3$ | 222−233 | GPQITSPALTQL | 0.4637 | NA | EM |
| | epitope CTL | $E_1$ | 35−43 | RPLAAAGIV | 0.4797 | NA | EM |
| | | $E_2$ | 205−213 | QVGVELSLY | 0.8613 | NA | EM |
| | | $E_3$ | 212−220 | LYLTELTTV | 0.8958 | NA | EM |
| | | $E_4$ | 227−235 | SPALTQLTI | 0.9003 | NA | EM |
| | | $E_5$ | 240−248 | NLAGSNMDY | 0.8480 | NA | EM |
| | | $E_6$ | 245−253 | NMDYLLTKL | 0.7282 | NA | EM |
| | | $E_7$ | 300−308 | ATYLETLSV | 0.4129 | NA | EM |
| | | $E_8$ | 379−387 | LTTPYLTLK | 0.7754 | NA | EM |
| | | $E_9$ | 383−391 | YLTLKGSVI | 0.6714 | NA | EM |
| | | $E_{10}$ | 427−435 | LSLDGITLR | 0.8224 | NA | EM |
| | | $E_{11}$ | 428−436 | SLDGITLRL | 0.5295 | NA | EM |
| | | $E_{12}$ | 504−512 | YIVLTVVSL | 1.2955 | NA | EM |
| | | $E_{13}$ | 505−513 | IVLTVVSLV | 1.1583 | NA | EM |
| | | $E_{14}$ | 506−514 | VLTVVSLVF | 0.9971 | NA | EM |
| | | $E_{15}$ | 517−525 | LSLVLICYL | 1.2555 | NA | EM |
| | | $E_{16}$ | 518−526 | SLVLICYLM | 0.8804 | NA | EM |
| | | $E_{17}$ | 519−527 | LVLICYLMY | 0.7853 | NA | EM |
| | | $E_{18}$ | 536−544 | LLWLGNNTL | 0.4064 | NA | EM |
| | epitope HTL | $E_1$ | 34−48 | GRPLAAAGIVVTGDK | 0.4569 | NA | EM |
| | | $E_2$ | 35−49 | RPLAAAGIVVTGDKA | 0.5427 | NA | EM |
| | | $E_3$ | 126−139 | ALGVATAAQITAAAA | 0.8498 | NA | EM |
| | | $E_4$ | 318−332 | LVPKVVTQVGSVIEE | 0.4500 | NA | EM |
| | | $E_5$ | 532−546 | QQKTLLWLGNNTLDQ | 0.4601 | NA | EM |
| protein HN | epitope B | $E_1$ | 161−170 | NFIPAPTTGS | 0.7259 | NA | EM |
| | | $E_2$ | 280−292 | QYHEKDLDVITLF | 0.7614 | NA | EM |
| | epitope CTL | $E_1$ | 95−103 | ALLSTESVI | 0.5043 | NA | EM |
| | | $E_2$ | 132−140 | YIGGIGKEL | 0.7564 | NA | EM |
| | | $E_3$ | 148−156 | VTSFYPSAF | 0.4192 | NA | EM |
| | | $E_4$ | 177−185 | SFDISATHY | 1.7398 | NA | EM |
| | | $E_5$ | 273−281 | GRLGFDGQY | 1.9611 | NA | EM |
| | | $E_6$ | 274−282 | RLGFDGQYH | 1.3727 | NA | EM |
| | | $E_7$ | 281−289 | YHEKDLDVI | 1.3509 | NA | EM |
| | | $E_8$ | 397−405 | LMGAEGRVL | 0.4415 | NA | EM |
| | | $E_9$ | 405−412 | LTVGTSHFL | 0.6614 | NA | EM |
| | | $E_{10}$ | 406−413 | TVGTSHFLY | 0.5265 | NA | EM |
| | | $E_{11}$ | 418−426 | SSYFSPALL | 0.7036 | NA | EM |
| | | $E_{12}$ | 419−427 | SYFSPALLY | 0.6322 | NA | EM |
| | | $E_{13}$ | 468−476 | GVYTDPYPL | 0.6599 | NA | EM |
| | | $E_{14}$ | 469−477 | VYTDPYPLV | 0.6099 | NA | EM |
| | | $E_{15}$ | 470−478 | YTDPYPLVF | 1.0589 | NA | EM |
| | | $E_{16}$ | 551−559 | TLFGEFRIV | 0.4567 | NA | EM |
| | | $E_{17}$ | 557−565 | RIVPLLVEI | 1.1852 | NA | EM |
| | epitope HTL | $E_1$ | 157−171 | QEHLNFIPAPTTGSG | 0.9029 | NA | EM |
| | | $E_2$ | 221−235 | FSTLRSINLDDNQNR | 0.6869 | NA | EM |
| | | $E_3$ | 475−489 | PLVFHRNHTLRGVFG | 0.5237 | NA | EM |
| | | $E_4$ | 555−569 | EFRIVPLLVEILKDG | 0.7710 | NA | EM |

[a]NA = nonallergenic; EM = exomembranous.

immunity conferred have yet to be studied. These prospective studies are essential to assess the viability of this prototype vaccine. However, they require substantial financial resources and a long phase of experimentation on animals to assess all the steps of design. Given the persistence of ND in Madagascar and its significant impact on poultry farming,[15] it is imperative to explore alternative approaches to accelerate vaccine research while reducing the costs associated with animal experimentation,[16] and respecting the rule of 3R on animal experimentation.[17]

At present, the use of immunoinformatics methods shows promising potential for the modern design of new vaccines. This approach significantly reduces the number of required experiments *in vitro* and *in vivo*, thereby cutting the time and costs associated with vaccine development.[18] In a previous study, we identified immunogenic epitopes in the F and HN proteins of 12 NDV strains isolated in Madagascar, paving the



https://doi.org/10.1021/acsomega.4c09890
ACS Omega 2025, 10, 4007−4018

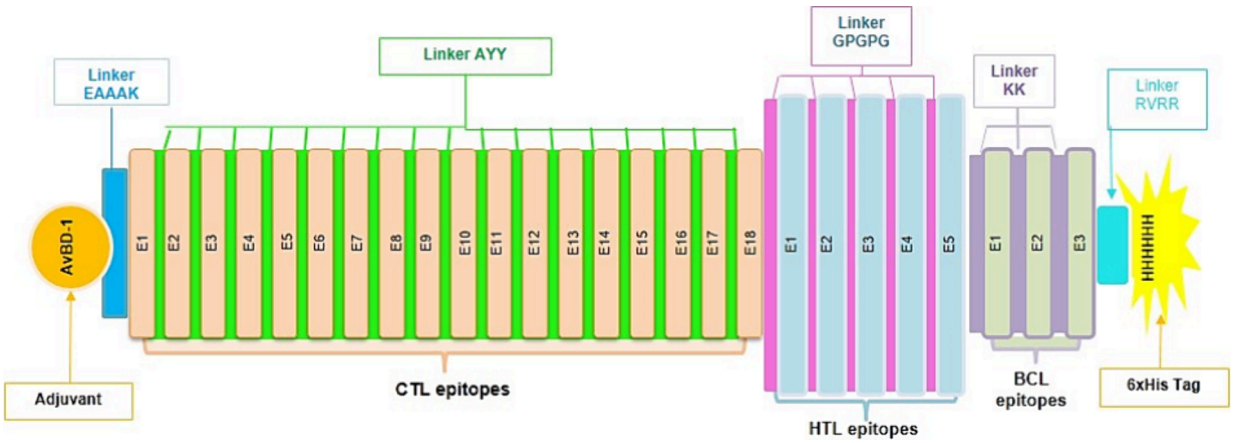


**Figure 1.** Structure of *MEV*-NDV_F multi-epitope vaccine. The vaccine is composed of 26 epitopes. These epitopes are linked with linker AYY (green), GPGPG (dark blue), and linker KK (gray). The AvBD-1 adjuvant is linked to the N-terminus (green) via the EAAAK linker (light blue). A "6xHis" tag has been added to the C-terminus of the vaccine construct via the RVRR linker (turquoise).

way for the design of multi-epitope vaccines.[19] Thus, the objectives of the present study are to apply immunoinformatics in the design of multi-epitope vaccines (MEV) based on those epitopes identified in the F and HN proteins of NDV isolated in Madagascar, and to evaluate the efficacy of the designed MEV. In evaluating the efficacy of MEV, various parameters such as antigenicity, allergenicity, solubility and physicochemical properties are studied. In addition, the affinity of MEV with host cell receptors such as the chicken TLR and their ability to induce a cellular response are also studied.

## 2. RESULTS

**2.1. Selection of Conserved Epitopes.** Of the 120 epitopes analyzed, 26 F protein epitopes (3 BCL epitopes, 18 CTL epitopes and 5 HTL epitopes) and 22 HN protein epitopes (2 BCL epitopes, 17 CTL epitopes and 3 HTL epitopes) are conserved in all aligned sequences (Figure S1). Information on these conserved epitopes is summarized in Table 1.

**2.2. Structure of Multi-epitope Vaccines.** Two multi-epitope vaccines, encoded *MEV*-NDV_F and *MEV*-NDV_HN, were formulated by integrating 26 conserved F protein epitopes and 22 conserved HN protein epitopes, respectively. Epitopes were assembled using AYY, GPGPG and KK linkers, as illustrated in Figure 1. The AvBD-1 adjuvant was specifically attached to the N-terminus of the first CTL epitope in each vaccine formulation, via the EAAAK linker. The remaining CTL epitopes were linked together with the AYY linker. In addition, the first HTL epitope was linked to the last CTL epitope via the GPGPG linker. The first B epitope was also linked to the last HTL epitope via the KK linker, while the remaining B epitopes were assembled with the KK linker.

**2.3. Physicochemical Properties, Antigenicity, and Allergenicity of the MEV.** The physicochemical properties of the designed MEV are summarized in Table 2. *MEV*-NDV_F is characterized by a longer amino acid chain and correspondingly higher molecular weight than *MEV*-NDV_HN. Both MEV have a slightly basic theoretical isoelectric point. Their stability is confirmed by instability indices below the threshold value. *MEV*-NDV_F exhibits a higher aliphatic index and a positive GRAVY, indicating less hydrophilicity than *MEV*-NDV_HN, which is characterized by a negative GRAVY, revealing greater hydrophilicity. Both MEV

**Table 2. Physicochemical Properties of Multi-Epitope Vaccines**[a]

| vaccine properties | threshold values | *MEV*-NDV_F | *MEV*-NDV_HN |
|---|---|---|---|
| number of amino acids | | 430 | 388 |
| molecular weight (Da) | 110 000 | 46820.97 | 43966.26 |
| theoretical isoelectric point (pI) | 7 (pH neuter) | 9.29 | 8.79 |
| aliphatic indices | | 112.56 | 83.51 |
| instability indicators (II) | 40 | 31.15 | 34.20 |
| estimated half-life in mammalian reticulocytes | | 30 h | 30 h |
| estimated half-life in yeast | | >20 h | >20 h |
| estimated half-life in *E. coli* | | >10 h | >10 h |
| grand average hydropathy index (GRAVY) | 0 | 0.420 | −0.013 |
| protein solubility (Web Protein-Sol) | 0.45 | 0.485 | 0.243 |
| antigenicity (VaxiJen v2.0) | 0.4 | 0.6400 | 0.6547 |
| allergenicity (AllerTOP v2.0) | | NA | NA |

[a]NA = nonallergenic.

show an estimated half-life of 30 h in mammalian reticulocytes (*in vitro*), over 20 h in yeast (*in vivo*) and over 10 h in *Escherichia coli* (*in vivo*). *MEV*-NDV_F and *MEV*-NDV_HN, show high antigenicity scores, exceeding the threshold of 0.4, indicating their robust antigenic potential. Finally, the AllerTOP server result confirms the absence of allergenic potential for these two MEV.

**2.4. Prediction, Refinement, and Evaluation of the 3D Structure of Multi-epitope Vaccines.** After refinement in GalaxyRefine server, five refined models of *MEV*-NDV_F and five refined models of *MEV*-NDV_HN were retained (Table 3). Of these, models n°4 were identified as the most accurate in terms of structure (Table 3 and Figure 2A). These models are distinguished by high GDT-HA scores, indicating high accuracy of the structure backbone. In addition, they exhibit reduced RMSD values, suggesting strong conformity with better spatial resolution. Their structural stability is confirmed by low MolProbity scores (2.055 for *MEV*-NDV_F and 2.583 for *MEV*-NDV_HN), indicating optimal stereochemical quality (Table 3). Consequently, they were selected for further analysis.



https://doi.org/10.1021/acsomega.4c09890
ACS Omega 2025, 10, 4007−4018

**Table 3. List of Models and Scores Obtained by the GalaxyRefine Server**

| name of MEV | model | GDT-HA | RMSD | MolProbity |
|---|---|---|---|---|
| *MEV*-NDV_F | model 1 | 0.9948 | 0.239 | 2.090 |
| | model 2 | 0.9953 | 0.240 | 2.102 |
| | model 3 | 0.9942 | 0.242 | 2.130 |
| | model 4 | 0.9971 | 0.231 | 2.055 |
| | model 5 | 0.9953 | 0.248 | 2.105 |
| *MEV*-NDV_HN | model 1 | 0.9704 | 0.363 | 2.525 |
| | model 2 | 0.9639 | 0.384 | 2.459 |
| | model 3 | 0.9568 | 0.390 | 2.603 |
| | model 4 | 0.9723 | 0.357 | 2.583 |
| | model 5 | 0.9671 | 0.378 | 2.484 |

Validation of selected models generated the plots shown in Figure 2, which reveal that the MEV *Z*-scores are −2.98 and −2.21 for *MEV*-NDV_F and *MEV*-NDV_HN respectively (Figure 2B). Analysis of the Ramachandran plot of the refined *MEV*-NDV_F model revealed that 97.8% of the residuals were in the permitted region and only 2.2% in the unpermitted region. For the *MEV*-NDV_HN refined model, 97.2% of the residues were in the authorized region, and only 2.8% of the residues in the unauthorized regions (Figure 2C). These results suggest that the overall and stereochemical qualities of the refined 3D structures of these two MEV were satisfactory.

In contrast, AlphaFold3 server generated only five models for *MEV*-NDV_F and five models for *MEV*-NDV_HN. Nevertheless, the ipTM and pTM scores of these models are below the threshold of 0.5, indicating that their quality is relatively low (Figure S2). Despite this, the models with an ipTM score of 0.16 for *MEV*-NDV_F and an ipPTM score of 0.22 for *MEV*-NDV_HN were chosen for molecular docking studies with TLR7.

**2.5. Analysis of Multi-epitope Vaccine Docking with TLR7.** The ClusPro v2.0 server produced 30 model complexes with their respective members and corresponding energy weight scores (Table S1). Of these, model n°4 of the *MEV*-NDV_F*TLR7 complex (with an energy weight score of −1179.1 kcal/mol and 24 members) and model n°7 du *MEV*-NDV_HN*TLR7 of the *MEV*-NDV_HN*TLR7 (with an energy weight score of −1516.1 kcal/mol and 19 members) represent the best-anchored complexes. In fact, they have lower energy weight scores and a higher number of cluster members. The results obtained in the PRODIGY server and PDBsum revealed that both MEV establish stronger interactions with TLR7, as evidenced by negative values of the Gibbs free energy $\Delta G$, lower values of the dissociation constant $K_d$ and the presence of hydrogen bonds, salt bridges and unbound contacts (Table 4 and Figure 3).

For the AlphaFold3 server, five models of *MEV*-NDV_F*TLR7 complexes and five models of *MEV*-NDV_HN*TLR7 complexes were generated. Among these,

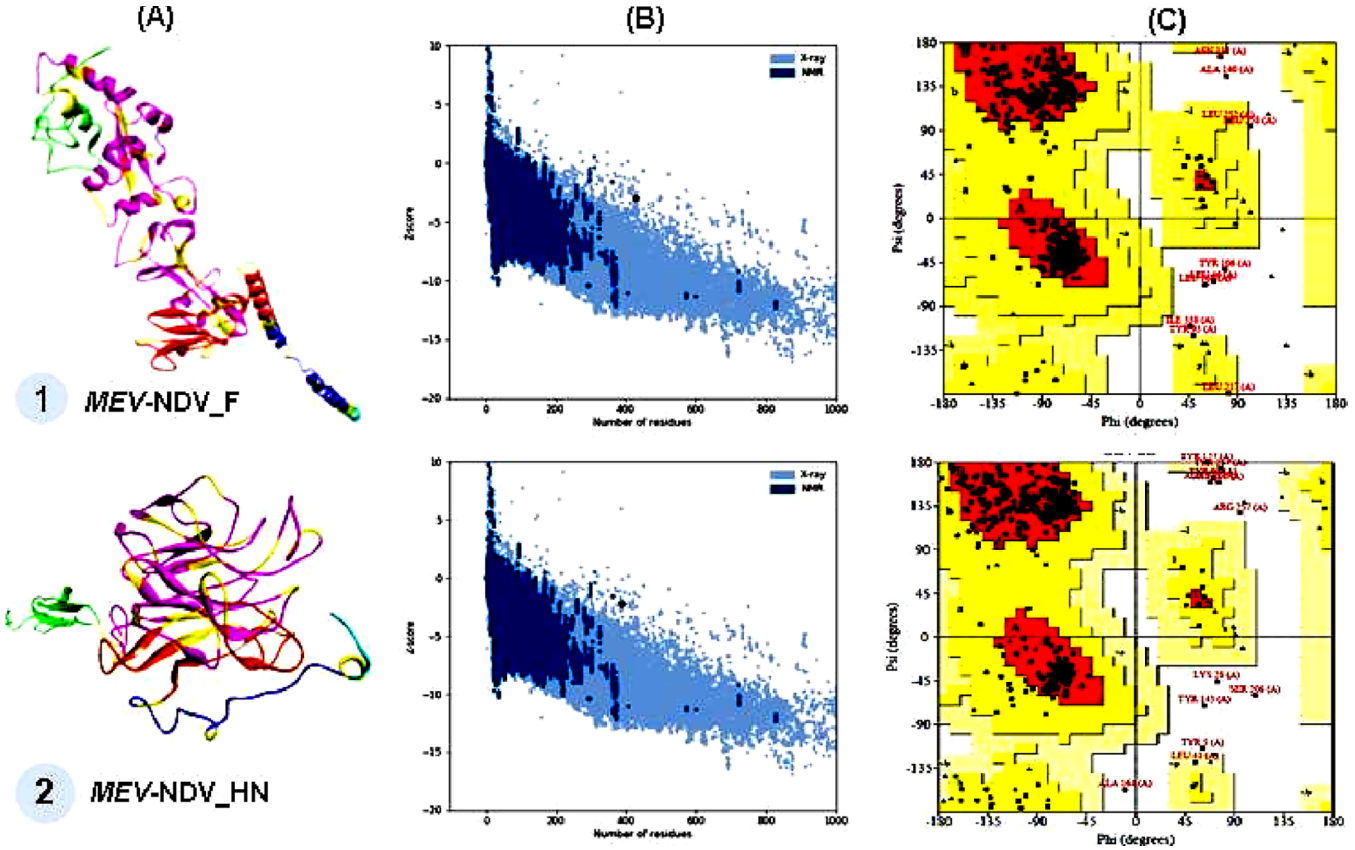


**Figure 2.** 3D structures of the MEV and results of the validation of the structures: (A) Refined 3D structures of the MEV. In this structure, the red and blue colors correspond to the CTL, HTL, and B epitopes, respectively, while the green, yellow, and cyan colors represent the adjuvant, linkers, and 6xHis tag, respectively. (B) *Z*-score plot of refined 3D structures predicted by the ProSA-Web server. (C) Ramachandran plots of the refined 3D structures generated by the PROCHECK server: Red regions represent the most favored regions, dark yellow regions represent additional authorized regions, light yellow regions represent generally authorized regions, and white regions represent unauthorized regions.



https://doi.org/10.1021/acsomega.4c09890
ACS Omega 2025, 10, 4007−4018

**Table 4. Binding Affinities of Multi-Epitope Vaccines to the TLR7 Receptor, Based on the PRODIGY Server and PDBsum**

| protein complexes | *MEV*-NDV_F*TLR7 | | *MEV*-NDV_HN*TLR7 | |
|---|---|---|---|---|
| docked proteins | TLR7 | *MEV*-NDV_F | TLR7 | *MEV*-ND_HN |
| number of residues in the interface | 40 | 35 | 43 | 41 |
| interface area (Å2) | 2060 | 2213 | 2224 | 2292 |
| interaction energy $\Delta G$ (kcal·mol$^{-1}$) | −20.6 | | −20.8 | |
| number of salt bridges | 1 | | 5 | |
| number of disulfide bonds | | | | |
| number of hydrogen bonds | 24 | | 30 | |
| number of unrelated contacts | 260 | | 284 | |

models n°1 and n°0 were selected for *MEV*-NDV_F*TLR7 and *MEV*-NDV_HN*TLR7, respectively, due to their higher iPTM and pTM scores (ipTM = 0.3 and pTM = 0.64). Results obtained from predictions using the Prodigy and PDBsum servers also confirmed that the MEV interact strongly with TLR7 (Figure S3).

**2.6. Molecular Dynamics Simulation.** Molecular dynamics simulation results for the MEV-TLR7 complex reveal that all docked complexes exhibit considerable deformability values, illustrating that most residues in the complex undergo deformation and show movement relative to their initial position (Figure 4A). The B-factor values of all complexes are high, which also correlates with the deformability of the complexes (Figure 4B,C). The eigenvalues of all complexes initially show the lowest values but increase progressively in each mode. This suggests that less energy is required to deform the structures, which correlates with efficient binding (Figure 4D). The variance associated with each normal mode is inversely proportional to the eigenvalue. Analysis of the variance plot showed a sudden or moderate decrease in the individual variance of each consecutive mode (Figure 4E).

Taken together, molecular dynamics analysis clearly demonstrated that MEV-TLR complexes exhibited high deformability and displayed acceptable eigenvalues, indicating efficient and uniform binding between MEV and TLR.

**2.7. Immune Simulation Result for Multi-epitope Vaccines.** Immune simulation results showed increased levels of macrophages (MA), dendritic cells (DC) and natural killer (NK) cells following administration of first and second doses of each formulated MEV (Figure 5a−c). A similar result was

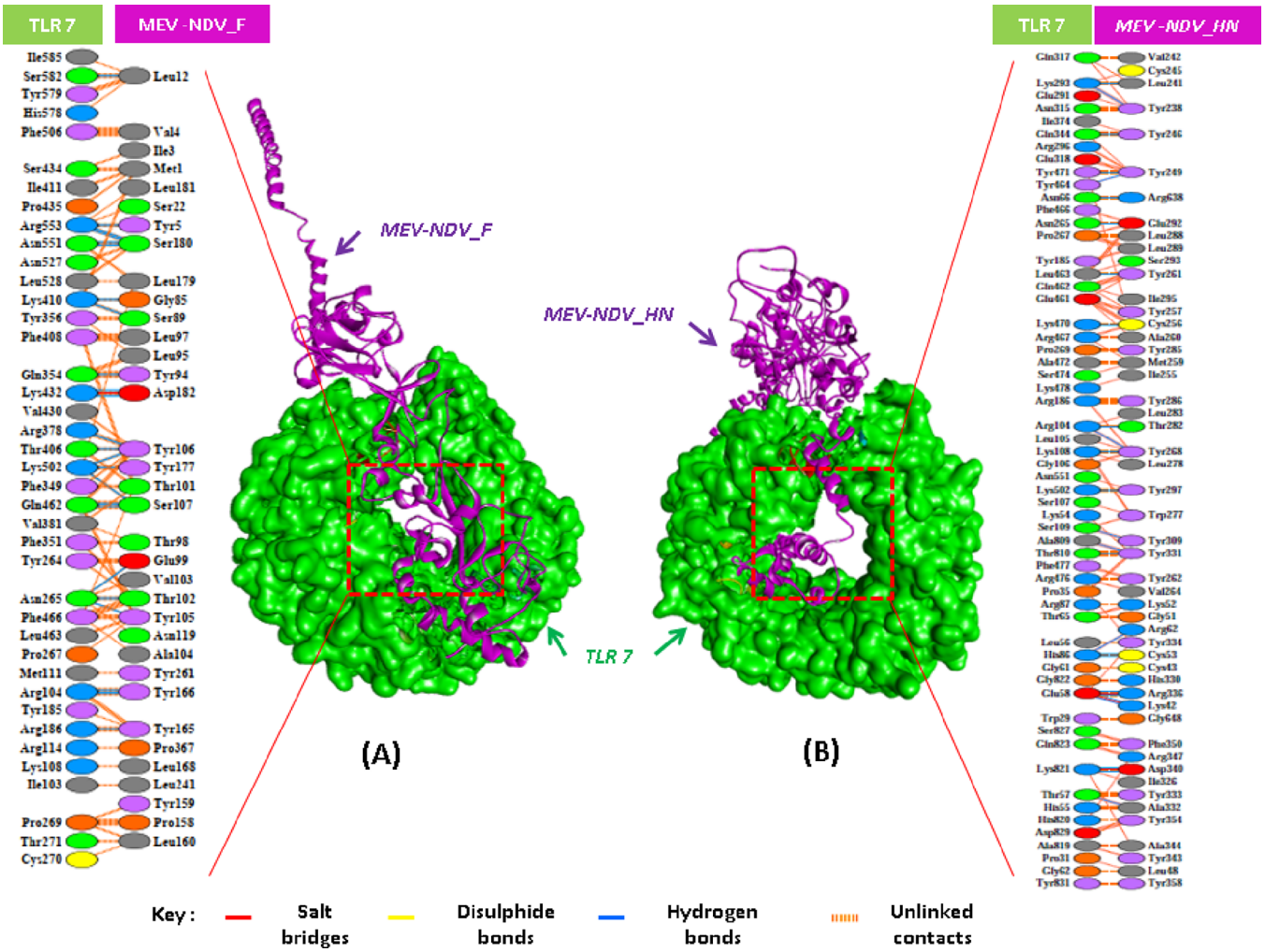


**Figure 3.** Representation of MEV-TLR7 complexes and interacting residues predicted by PDBsum: (A) *MEV*-NDV_F*TLR7 complex and interacting residues predicted by PDBsum; (B) *MEV*-NDV_HN*TLR7 complex and interacting residues predicted by the PDBsum server.



https://doi.org/10.1021/acsomega.4c09890
*ACS Omega* 2025, 10, 4007−4018

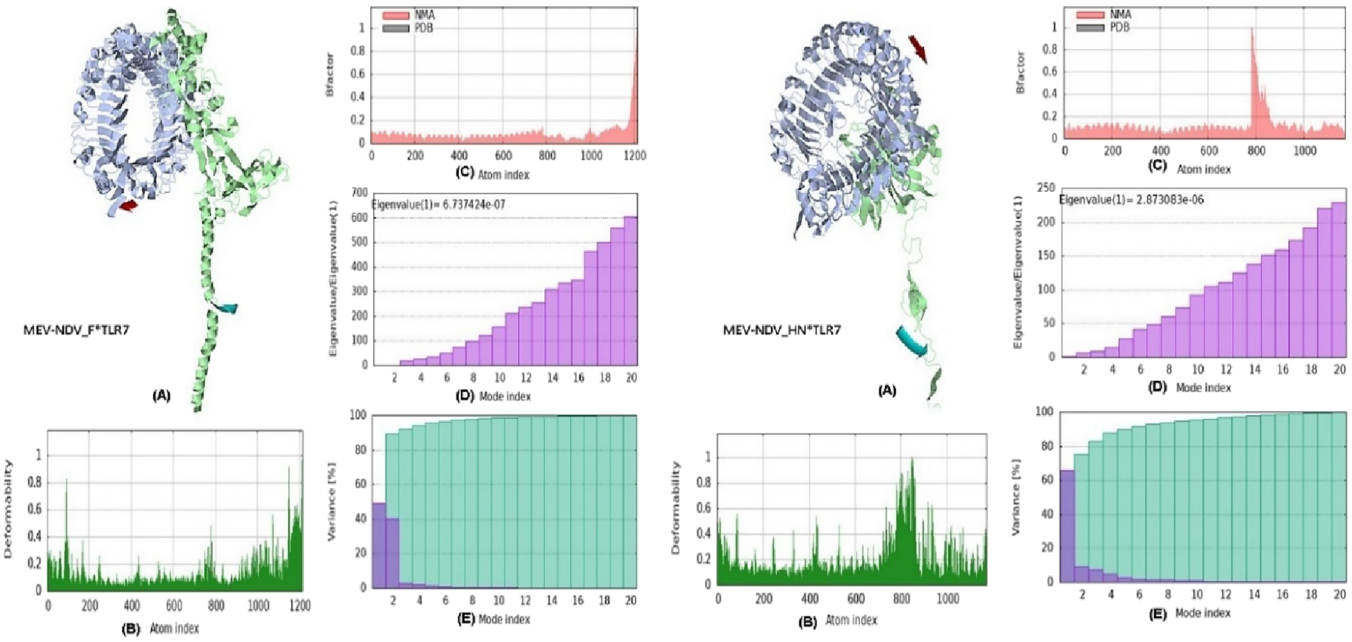


**Figure 4.** Molecular dynamics simulation presentation of the *MEV*-NDV_F*TLR7 and *MEV*-NDV_HN*TLR7 complexes: (A) Direction of movement is indicated by red and cyan. (B) Vaccine stability was analyzed by the low deformability of the main chain. (C) B factor. (D) The eigenvalue demonstrates the protein's normal mode and rigidity of movement. (E) Mode variance.

shown for IFN-$\gamma$ and IL-2 levels (Figure 5d). These results suggest an active innate immune response, favoring elimination of the administered antigen and activation of humoral and cellular responses. This is justified by the decrease in antigen concentration after a few days of administration (Figure 5i).

An increase in the production of memory B cells, IgM isotype-producing B cells, plasma cells, TH-cells and their Th-1 subpopulations, as well as TC-cells, were also found after first and second doses of MEV (Figure 5e−h). These results suggest the activation of a postvaccination humoral and cellular immune response.

IgM antibody titer is also increased during the primary response (after administration of the first dose), with levels below 50,000 (Figure 5i). However, increases in IgM antibody titer (above 250,000), IgG1 + IgG2 (above 50,000) and IgM + IgG immune complex (above 350,000) were observed in secondary responses (i.e., after administration of the second dose). These results indicate the presence of postvaccination seroconversion in the vaccinated organism following the administration of MEV. They also suggest that the MEV designed in this study are likely to be highly immunogenic.

## 3. DISCUSSION

This study involved the design of two multi-epitope vaccines containing conserved epitopes of F and HN proteins from 12 strains isolated from Madagascar, which belong to genotype XI.[14] The MEV were developed using immunoinformatics approaches, and the immune responses they elicited were assessed by *in silico* immune simulations. Similar research has been carried out in Pakistan[20] and in Iran,[21] but with a different approach: these studies focused solely on HN or F proteins. In contrast, our study took a novel approach by simultaneously targeting F and HN proteins, which is crucial for improving vaccine efficacy by targeting two key components of the virus. However, we separated the epitopes of the F and HN proteins, enabling in-depth analysis of the immune responses induced by each of these proteins. This approach offers us a valuable perspective for the selection of vaccine formulations adapted to the specific epidemiological needs of Madagascar.

The constructed MEV contain conserved CTL, HTL and BCL epitopes of the F and HN proteins (Table 1). These epitopes are linked using the AAY, GPGPG and KK linkers respectively (Figure 1). The AAY linker is specifically chosen to unite CTL epitopes, due to its ability to prevent junctional epitope formation and enhance antigenic presentation.[22] In addition, the GPGPG linker is used to link HTL epitopes because of its ability to induce T helper cell responses.[23] The KK linker is used to link BCL epitopes. This choice is motivated by the fact that the KK linker is the target of Cathepsin B, a lysosomal protease involved in the processing of antigenic peptides for presentation at the cell surface in MHC-II-restricted antigen presentation.[24]

In general, MEV are less immunogenic than conventional vaccines. To improve their immunogenicity, the adjuvant AvBD-1, an antimicrobial and immunomodulatory agent,[25] has been added to the N-terminus of MEV formulations, according to Martinelli.[26] It is linked to the first CTL epitope using the EAAAK linker. This rigid peptide linker ensures effective separation between the functional domains of the adjuvant and the epitopes, preserving their individual functional properties.[27] To facilitate postexpression purification, a 6xHis tag has been added to the proposed vaccine proteins at these C-terminal regions.[28]

The two MEV designed are antigenic, nonallergenic and have 430 and 388 amino acid residues respectively. These sizes would not be a problem in terms of efficacy, stability or expression.[29] In addition, they were significantly basic, stable, thermostable and hydrophilic (Table 2).

Appropriate interactions between a vaccine and target immune cells are essential to induce an effective immune response. Accordingly, a molecular docking study was performed to assess the binding of MEV to the TLR7 immune


https://doi.org/10.1021/acsomega.4c09890
ACS Omega 2025, 10, 4007−4018

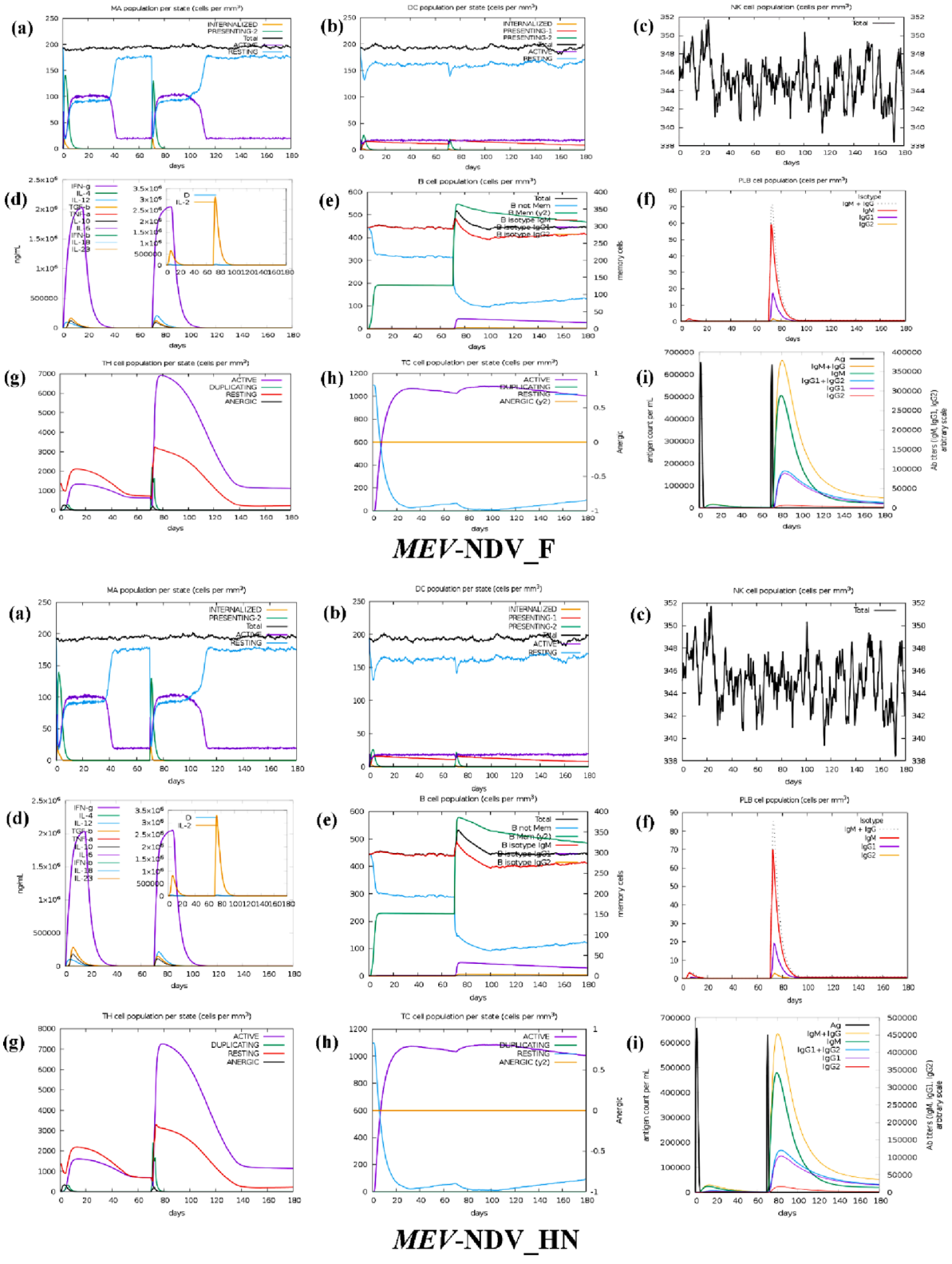


**Figure 5.** Immune simulation of *MEV*-NDV_F and *MEV*-NDV_HN after both antigen injections. (a) MA macrophage population. (b) DC dendritic cell population. (c) NK natural killer cell populations. (d) Induced cytokine secretion and IL-2 levels. (e) B-cell populations (memory and nonmemory B-cells and B-cell isotypes). (f) Plasma cell populations. (g) TH active and TH-cell populations. (h) TC active and TC-cell populations. (i) Antibody production in response to antigen injections, where antibodies are represented by different colors and the antigen is shown in black.

receptor. This receptor was chosen because of its key role in antiviral immunity, particularly against single-stranded RNA viruses.[30] It is also present on the surface of plasmacytoid dendritic cells, B cells, eosinophils, neutrophils, and monocytes/macrophages, making it an important target for vaccine and therapeutic research.[31,32] The results of this study revealed



https://doi.org/10.1021/acsomega.4c09890
ACS Omega 2025, 10, 4007−4018

Table 5. List of Sequences Downloaded from NCBI

| no. | strains | ID number | | collection date | references |
|---|---|---|---|---|---|
| | | F proteins | HN proteins | | |
| 1 | MG-1992 | ADQ64395 | ADQ64396 | 1992 | 14 |
| 2 | MG-725 | ADQ64389 | ADQ64390 | 2008 | 14 |
| 3 | MG-MEOLA | ADQ64398 | ADQ64399 | 2008 | 14 |
| 4 | MG-39 | ADQ64401 | ADQ64402 | 2008 | 14 |
| 5 | MGMNJ | AGC23353 | AGW43230 | 2009 | 41 |
| 6 | MGF003C | AGC23347 | AGW43224 | 2010 | 41 |
| 7 | MGF082T | AGC23349 | AGW43226 | 2010 | 41 |
| 8 | MGF015C | AGC23348 | AGW43225 | 2011 | 41 |
| 9 | MGF120T | AGC23350 | AGW43227 | 2011 | 41 |
| 10 | MGF166 | AGC23351 | AGW43228 | 2011 | 41 |
| 11 | MGF192C | AGC23352 | AGW43229 | 2011 | 41 |
| 12 | MGS1130T | AGC23354 | AGW43231 | 2011 | 41 |

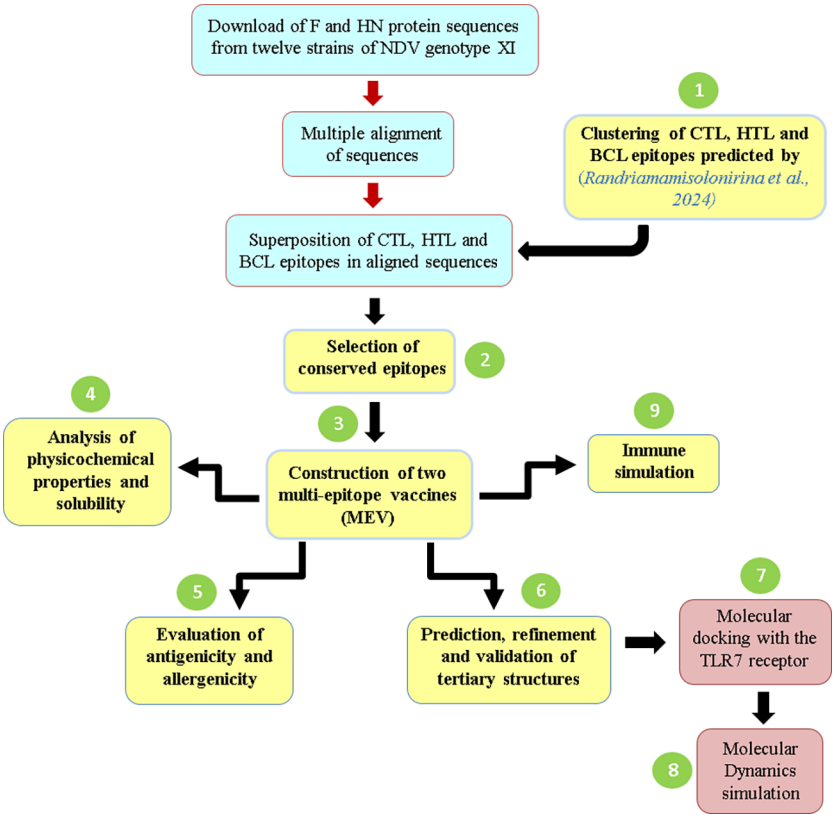


**Figure 6.** Schematic diagram illustrating the overall steps in the immunoinformatics analysis carried out in this study.

robust interactions between MEV and TLR7. This was confirmed by the negative values of the Gibbs free energy $\Delta G$, the lower values of the dissociation constant $K_d$, as well as the presence of hydrogen bonds, salt bridges and unbound contacts in the molecular interactions (Table 4 and Figure 3). By interacting with TLR7, these vaccines can stimulate these cells, promote production of cytokine and accelerate the mobilization of effector cells, leading to humoral and cellular responses.[33]

Molecular dynamics simulations were performed to understand the stability of the vaccine construct when in complex with TLR receptors. The analysis revealed high atomic deformability, with acceptable eigenvalues, suggesting efficient and uniform binding between the MEV and the TLR.

Computer simulation of MEV-induced immune responses showed increased levels of macrophages, NK cells, dendritic cells (DC), T helper and T cytotoxic lymphocytes, memory B lymphocytes and plasma cells. Elevated production of IFN-$\gamma$ and IL-2 was also found (Figure 5d). In addition, increased release of IgM, IgG and their isotypes is also observed (Figure 5i). On the one hand, elevated levels of IFN-$\gamma$ and IL-2 correlate positively with increased levels of activated immune cells such as T helper lymphocytes and NK cells.[34,35] It has also been suggested that IFN-$\gamma$ and IL-2 are involved in early host defense, contribute to T cell differentiation and are involved in cytotoxicity and antibody production.[36,37] This is why they are produced in large quantities after each dose of vaccine.


https://doi.org/10.1021/acsomega.4c09890
ACS Omega 2025, 10, 4007−4018

In addition, these results demonstrate the ability of MEV to stimulate the innate and adaptive immune systems (encompassing both humoral and cellular responses) of vaccinated organisms. These stimulations then promote the development of memory cells and increase antibody production. Indeed, vaccines containing viral antigens are recognized by antigen-presenting cells such as macrophages and dendritic cells. Macrophages then present vaccine epitopes and activate T helper via MHC-II molecules, inducing adaptive immunity and activating B cells to generate humoral immunity. At the same time, dendritic cells can cross-present CTL epitopes, activating T cytotoxic lymphocytes and facilitating cellular immunity.[28,38] In this way, the newly formulated MEV can serve as a basis for the manufacture of subunit or recombinant vaccines, thereby contributing to the development of new-generation vaccines against ND in the future.

As this is an immunoinformatics study based on *in silico* methods, the epitopes identified in the formulation and the results of the simulations need to be validated by experimental *in vitro* and/or *in vivo* analyses before any further application. In addition, the number of protein sequences analyzed is still limited and the arrangement of epitopes in vaccine formulations to achieve a more stable 3D structure has not yet been investigated. Consequently, further bioinformatics studies are also needed to explore this possibility.

## 4. CONCLUSIONS

This study utilizes immunoinformatics methods to design two multi-epitope vaccines against Newcastle disease. The neo-synthesized vaccines were found to be highly antigenic, nonallergenic and physico-chemically stable. Molecular docking studies, combined with molecular dynamics simulations demonstrated a high affinity and stable interaction between these vaccines and the TLR7 receptor of immune cells. In addition, immune response simulations demonstrated the ability of these vaccines to induce the immune responses required for vaccine immunity, as well as to promote efficient memory cell development. These findings suggest that immunoinformatics-designed multi-epitope vaccines could serve as a promising foundation for a new recombinant or subunit vaccine against Newcastle disease. However, experimental validation through *in vitro* and *in vivo* studies is essential to assess the safety and efficacy of the proposed vaccines. Furthermore, additional bioinformatics research is needed to explore the optimal arrangement of epitopes within vaccine formulations to enhance their stability and immunogenicity.

## 5. MATERIALS AND METHODS

Figure 6 shows a diagram summarizing the steps involved in multi-epitope vaccine design.

**5.1. Data Preparation.** The 120 epitopes previously identified by our team as potentially effective for vaccines design were used in the present study. These epitopes have previously been identified using immunoinformatics methods and were found in the 12 F protein sequences and 12 HN protein sequences of NDV isolated in Madagascar.[19]

**5.2. Identification of Conserved Epitopes.** To identify the conserved epitope among the 120 epitopes, a multiple sequence alignment was performed. To this end, the 24 F and HN protein sequences were extracted from the NCBI protein database (http://www.ncbi.nlm.nih.gov/protein) in FASTA format (Table 5). Then, they were aligned in BioEdit software version 7.0.5.3,[39] using the Clustal W program.[40] In the alignment, the F and HN protein sequences of strain MG-1992[14] were taken as references. Afterward, the 120 epitopes were positioned in the aligned sequences, and the epitopes found in all the aligned and nonmutated sequences were considered as conserved epitopes and retained for the rest of the study.

**5.3. Formulation of the Multi-epitope Vaccine.** In this study, two MEV, namely *MEV*-NDV_F and *MEV*-NDV_HN were formulated using F and HN protein epitopes, respectively. In the formulation, CTL epitopes were joined with AAY linkers, while HTL epitopes and B epitopes were linked with GPGPG and KK linkers, respectively.[42] In addition, avian $\beta$-defensin (AvBD-1, GenBank accession number: NP_990324), an adjuvant of 65 amino acids was incorporated into the N-terminus of each construct via the EAAK linker.[20] Finally, the "6xHis tag" was also added to the C-terminus of each vaccine construct via the RVRR linker.[28]

**5.4. Assessment of the Physicochemical Properties and Solubility of Designed MEV.** The Expasy-Prot Param server[43] was used to evaluate the physicochemical aspects of *MEV*-NDV_F and *MEV*-NDV_HN. For each vaccine formulation, amino acid compositions, molecular weight (MW, threshold = 110 kDa), theoretical isoelectric point (pI, threshold = 7 indicates neutral pH), instability index (II, threshold = 40), half-life, aliphatic index and GRAVY (grand mean of hydropathy index) were calculated. In addition, the solubility of vaccines was studied using Protein-Sol.[44]

**5.5. Evaluation of Antigenicity and Allergenicity of Engineered MEV.** Antigenicity testing is a crucial element in the vaccine development process. As such, the VaxiJen 2.0 server was used with a cutoff value of 0.4 to predict the antigenicity of formulated MEV.[45] To ensure that these MEV did not provoke allergic reactions, allergenicity was predicted using the AllerTOP server.[46]

**5.6. Prediction, Refinement, and Validation of the 3D Structure of the MEV.** The three-dimensional (3D) structure of the vaccines was first predicted using GalaxyWEB[47] and AlphaFold3[48] servers.

The GalaxyWEB server uses model-based approaches to predict the 3D structure of vaccines.[47] The raw 3D vaccine models obtained were then refined using the GalaxyRefine program.[49] This program reconstructs unreliable loops or termini in the raw models using *Ab initio* methods.[49] It generates five refined models, and the most accurate model was selected based on the basis of GDT-HA (Global Distance Test-High Accuracy), RMSD (Root-Mean-Square Deviation) and MolProbity scores. The final 3D structure of the vaccine was then validated using the *Z*-score via the ProSA-web server[50] and he Ramachandran plot in PROCHECK.[51] The *Z*-score reflects the overall quality of the model, with a positive *Z*-score indicating that the structure contains errors.[50] In addition, the Ramachandran plot checks the stereochemical quality of the structure.[51] In this plot, a better structure has more residues in the favored regions and fewer residues in the disallowed regions according to Ramachandran.

Meanwhile, AlphaFold3 server is based on a neural network method for predicting the 3D structures of the MEV.[48] For each prediction, five models are generated. The models with the highest pTM (predicted model score) and ipTM (predicted model interface score) are then selected for


https://doi.org/10.1021/acsomega.4c09890
ACS Omega 2025, 10, 4007−4018

subsequent analysis. The 3D structure final of the MEV was visualized using Discovery Studio Visualizer 2017.[52]

**5.7. Molecular Docking with Immune Cell Receptors.** In order to generate a persistent immunological response, MEV must interact with targeted immune cell receptors. To assess these interactions, a molecular docking analysis was carried out between the two MEV obtained and the Toll-like receptor 7 or TLR7 (PDB ID: 5gmf). To this end, the 3D structure of TLR7 was uploaded to RCSB-PDB[53] in PDB format. It was then corrected in Discovery Studio Visualizer 2017,[52] by deleting the B chains and other cocrystallized molecules. In fact, only the chain A is required for molecular docking.

Molecular docking was performed using ClusPro v2.0 server[54] and AlphaFold3 server.[55] On the ClusPro server, a total of 30 models were generated for each docking case, and the models with the highest membership and lowest energy-weighted scores were selected as the final models of the MEV-TLR complex. In contrast, the AlphaFold3 server generates five complex models, from which the ones with the highest ipTM and pTM values are selected.[55]

The selected models were then submitted to PRODIGY[56] to predict the interaction energy or Gibbs free energy ($\Delta G$) in thermodynamic terms between MEV and TLR. Additionally, PDBsum[57] was used to analyze the interacting residues between the complexes. The docking complexes were visualized using Discovery Studio Visualizer 2017.[52]

**5.8. Molecular Dynamics Simulation.** iMOD online server[58] was used to predict the atomic-level molecular behavior and characteristics of docked complexes using molecular dynamics simulation. In this server, dynamic parameters such as deformability factor, B-factor, eigenvalues and variance of docked complexes were calculated.[58] The best docked complexes based on the lowest docking energies were submitted to the iMOD web server and the binding affinity of MEV to immune cell receptors was analyzed.

**5.9. Immune Simulation.** To mimic the immune response and immunogenicity of MEV in the host, an *in silico* immune simulation was carried out using C-IMMSIM.[59] In reality, an interval of 10 weeks (70 days) between 2 vaccine injections is suggested for Newcastle disease vaccine in the area where the disease is severe.[60] Consequently, two injections were administered during the simulation. The first injection was administered 1 step after $J_0$, followed by the second injection set 210 steps after the first. The simulation was programmed over 540 steps, a time step equivalent to 8 h. As a result, the effect of the vaccine is monitored over a total period of 180 days (approximately 6 months). All other simulation parameters were set to default values.

## ■ ASSOCIATED CONTENT

### Supporting Information

The Supporting Information is available free of charge at https://pubs.acs.org/doi/10.1021/acsomega.4c09890.

Multiple sequence alignment of F and HN proteins from 12 NDV strains isolated in Madagascar and identification of conserved epitopes; 3D models of MEV using the AlphaFold3 server; analysis of molecular interactions between MEV and TLR7 with the AlphaFold3 server; results of multi-epitope vaccine (MEV) docking with Toll-like receptor 7 (TLR7) from the ClusPro v2.0 server (PDF)

## ■ AUTHOR INFORMATION


### Corresponding Author

**Natolotriniavo T. Randriamamisolonirina** − *Department of Research and Quality Control, Malagasy Institute of Veterinary Vaccines, Antananarivo BP 04, Madagascar;* orcid.org/0000-0001-5196-3737; Phone: (+261) 34 09 909 37; Email: randriamamisolonirina@gmail.com

### Authors

**Mirantsoa S. Razafindrafara** − *Department of Research and Quality Control, Malagasy Institute of Veterinary Vaccines, Antananarivo BP 04, Madagascar; Department of Zootechnical, Veterinary and Fish Research, National Center for Applied Research on Rural Development, Antananarivo BP 1690, Madagascar*

**Olivier F. Maminiaina** − *Department of Research and Quality Control, Malagasy Institute of Veterinary Vaccines, Antananarivo BP 04, Madagascar; Department of Zootechnical, Veterinary and Fish Research, National Center for Applied Research on Rural Development, Antananarivo BP 1690, Madagascar; Department of Veterinary Science and Medicine, Faculty of Medicine, University of Antananarivo, Antananarivo BP 566, Madagascar*

Complete contact information is available at: https://pubs.acs.org/10.1021/acsomega.4c09890


### Notes

The authors declare no competing financial interest.

## ■ ACKNOWLEDGMENTS

The authors would like to acknowledge IMVAVET for providing the infrastructure necessary to conduct this research. The authors received no financial support for the research or the publication of this article.

## ■ REFERENCES


(1) Dimitrov, K. M.; Abolnik, C.; Afonso, C. L.; Albina, E.; Bahl, J.; Berg, M.; Briand, F. X.; Brown, I. H.; Choi, K. S.; Chvala, I.; Diel, D. G.; Durr, P. A.; Ferreira, H. L.; Fusaro, A.; Gil, P.; Goujgoulova, G. V.; Grund, C.; Hicks, J. T.; Joannis, T. M.; Torchetti, M. K.; Kolosov, S.; Lambrecht, B.; Lewis, N. S.; Liu, H.; Liu, H.; McCullough, S.; Miller, P. J.; Monne, I.; Muller, C. P.; Munir, M.; Reischak, D.; Sabra, M.; Samal, S. K.; Servan de Almeida, R.; Shittu, I.; Snoeck, C. J.; Suarez, D. L.; Van Borm, S.; Wang, Z.; Wong, F. Y. K. Updated unified phylogenetic classification system and revised nomenclature for Newcastle disease virus. *Infect Genet Evol.* **2019**, *74*, No. 103917.

(2) Phale, S. Newcastle disease virus: Structural and molecular basis of pathogenicity. *Med. Chem.* **2018**, *08*, 202−204.

(3) Paldurai, A.; Kim, S. H.; Nayak, B.; Xiao, S.; Shive, H.; Collins, P. L.; Samal, S. K. Evaluation of the contributions of individual viral genes to newcastle disease virus virulence and pathogenesis. *J. Virol.* **2014**, *88* (15), 8579−96.

(4) Rao, P. L.; Gandham, R. K.; Subbiah, M. Molecular evolution and genetic variations of V and W proteins derived by RNA editing in Avian Paramyxoviruses. *Sci. Rep.* **2020**, *10* (1), 9532.

(5) Jin, J.; Zhao, J.; Ren, Y.; Zhong, Q.; Zhang, G. Contribution of HN protein length diversity to Newcastle disease virus virulence, replication and biological activities. *Sci. Rep.* **2016**, *6* (1), 36890.

(6) Mozafari, A.; Amani, J.; Shahsavandi, S.; Salmanian, A. H. A novel multi-epitope edible vaccine candidate for Newcastle disease virus: In silico approach. *Iran. J. Biotechnol.* **2022**, *20* (2), No. e3119.

(7) Dimitrov, K. M.; Afonso, C. L.; Yu, Q.; Miller, P. J. Newcastle disease vaccines - A solved problem or a continuous challenge? *Vet. Microbiol.* **2017**, *206*, 126−136.

(8) Maminiaina, O. F. *Caractérisation des virus de la maladie de Newcastle (APMV-1) circulant sur les haute terre de Madagascar*. PhD (Thèse de Doctorat d'Université), Département de Biochimie Fondamentale et Appliquée (DBFA)- Faculté des Sciences; Université d'Antananarivo: Antananarivo, 2011. https://theses.hal.science/tel-01561748 (accessed 2024−10−28).
(9) Miller, P. J.; Afonso, C. L.; El Attrache, J.; Dorsey, K. M.; Courtney, S. C.; Guo, Z.; Kapczynski, D. R. Effects of Newcastle disease virus vaccine antibodies on the shedding and transmission of challenge viruses. *Dev Comp Immunol.* **2013**, *41* (4), 505−513.
(10) Miller, P. J.; Estevez, C.; Yu, Q.; Suarez, D. L.; King, D. J. Comparison of viral shedding following vaccination with inactivated and live Newcastle disease vaccines formulated with wild-type and recombinant viruses. *Avian Dis.* **2009**, *53* (1), 39−49.
(11) Wajid, A.; Basharat, A.; Bibi, T.; Rehmani, S. F. Comparison of protection and viral shedding following vaccination with Newcastle disease virus strains of different genotypes used in vaccine formulation. *Trop Anim Health Prod.* **2018**, *50* (7), 1645−1651.
(12) Izquierdo-Lara, R.; Chumbe, A.; Calderón, K.; Fernández-Díaz, M.; Vakharia, V. N. Genotype-matched Newcastle disease virus vaccine confers improved protection against genotype XII challenge: The importance of cytoplasmic tails in viral replication and vaccine design. *PLoS One.* **2019**, *14* (11), No. e0209539.
(13) Randriamamisolonirina, T.; Maminiaina, O. F.; Razafindrafara, M. S.; Ramilijaona, V. M. Study of an inactivated Newcastle disease vaccine: clinical protection and immunogenicity. *ScienceOpen* Preprints. **2024**. .
(14) Maminiaina, O. F.; Gil, P.; Briand, F.-X.; Albina, E.; Keita, D.; Andriamanivo, H. R.; Chevalier, V.; Lancelot, R.; Martinez, D.; Rakotondravao, R.; Rajaonarison, J. J.; Koko, M.; Andriantsimahavandy, A. A.; Jestin, V.; Servan de Almeida, R.; Fooks, A. R. Newcastle Disease Virus in Madagascar: Identification of an original genotype possibly deriving from a died out ancestor of genotype IV. *PLoS One* **2010**, *5* (11), No. e13987.
(15) Maminiaina, O. F.; Koko; Ravaomanana, J.; Rakotonindrina, S. J. Epidémiologie de la maladie de Newcastle en aviculture villageoise à Madagascar. *Rev. Sci. Tech Off. Int. Epi.* **2007**, *26* (3), 691−700.
(16) Maria, R. A. R.; Arturo, C.-J. V.; Alicia, J.-A.; Paulina, M.-L. G.; Aparicio-Ozores, G. The Impact of bioinformatics on vaccine design and development. In *Vaccines*; Afrin, F.; Hemeg, H.; Ozbak, H., Eds. IntechOpen, 2017; p Ch. 7.
(17) Husain, A.; Meenakshi, D. U.; Ahmad, A.; Shrivastava, N.; Khan, S. A. A Review on alternative methods to experimental animals in biological testing: Recent advancement and current strategies. *J. Pharm. Bioallied Sci.* **2023**, *15* (4), 165−171.
(18) Oli, A. N.; Obialor, W. O.; Ifeanyichukwu, M. O.; Odimegwu, D. C.; Okoyeh, J. N.; Emechebe, G. O.; Adejumo, S. A.; Ibeanu, G. C. Immunoinformatics and vaccine development: An overview. *Immunotargets Ther.* **2020**, *9* (null), 13−30.
(19) Tendrinarisoa, R. N.; Suzanne, R. M.; Andriambandaina Abel, A.; Fridolin, M. O. Identification by immunoinformatics of the B and T epitopes in F and HN proteins of Newcastle disease viruses isolated in Madagascar. Preprints in *Research Square*. .
(20) Raza, A.; Asif Rasheed, M.; Raza, S.; Tariq Navid, M.; Afzal, A.; Jamil, F. Prediction and analysis of multi epitope based vaccine against Newcastle disease virus based on haemagglutinin neuraminidase protein. *Saudi Journal of Biological Sciences.* **2022**, *29* (4), 3006−3014.
(21) Hosseini, S. S.; Kolyani, K. A.; Tabatabaei, R. R.; Goudarzi, H.; Sepahi, A. A.; Salemi, M. In silico prediction of B and T cell epitopes based on NDV fusion protein for vaccine development against Newcastle disease virus. *Vet. Res. Forum.* **2021**, *12* (2), 157−165.
(22) Yang, Y.; Sun, W.; Guo, J.; Zhao, G.; Sun, S.; Yu, H.; Guo, Y.; Li, J.; Jin, X.; Du, L.; Jiang, S.; Kou, Z.; Zhou, Y. In silico design of a DNA-based HIV-1 multi-epitope vaccine for Chinese populations. *Hum Vaccin Immunother.* **2015**, *11* (3), 795−805.
(23) Livingston, B.; Crimi, C.; Newman, M.; Higashimoto, Y.; Appella, E.; Sidney, J.; Sette, A. A rational strategy to design multiepitope immunogens based on multiple Th lymphocyte epitopes. *T J. Immunol.* **2002**, *168* (11), 5499−5506.
(24) Yano, A.; Onozuka, A.; Asahi-Ozaki, Y.; Imai, S.; Hanada, N.; Miwa, Y.; Nisizawa, T. An ingenious design for peptide vaccines. *Vaccine* **2005**, *23* (17), 2322−2326.
(25) Zhang, G.; Sunkara, L. T. Avian Antimicrobial host defense peptides: From biology to therapeutic applications. *Pharmaceuticals.* **2014**, *7* (3), 220−247.
(26) Martinelli, D. D. In silico vaccine design: A tutorial in immunoinformatics. *Healthcare Analytics.* **2022**, *2*, No. 100044.
(27) Chen, X.; Zaro, J. L.; Shen, W.-C. Fusion protein linkers: Property, design and functionality. *Adv. Drug Deliv Rev.* **2013**, *65* (10), 1357−1369.
(28) Tan, C.; Zhu, F.; Pan, P.; Wu, A.; Li, C. Development of multi-epitope vaccines against the monkeypox virus based on envelope proteins using immunoinformatics approaches. *Front. Immunol.* **2023**, *14*, No. 1112816.
(29) Jamil, F.; Aslam, L.; Laraib; Ali, H.; Shoukat, K.; Rasheed, M. A.; Raza, S.; Ibrahim, M. An in silico study of derivative of Newcastle disease virus epitopes based vaccine against hemagglutunin neuraminidase protein. *J. Anim. Sci.* **2022**, *101*, No. skac375.
(30) Rehman, M. S.; Rehman, S. U.; Yousaf, W.; Hassan, F.-U.; Ahmad, W.; Liu, Q.; Pan, H. The potential of toll-like receptors to modulate Avian immune system: Exploring the effects of genetic variants and phytonutrients. *Front Genet.* **2021**, *12*, No. 671235.
(31) Sun, H.; Li, Y.; Zhang, P.; Xing, H.; Zhao, S.; Song, Y.; Wan, D.; Yu, J. Targeting toll-like receptor 7/8 for immunotherapy: recent advances and prospectives. *Biomark Res.* **2022**, *10* (1), 89.
(32) Dowling, D. J. Recent advances in the discovery and delivery of TLR7/8 agonists as vaccine adjuvants. *ImmunoHorizons.* **2018**, *2* (6), 185−197.
(33) Jeisy-Scott, V.; Kim, J. H.; Davis, W. G.; Cao, W.; Katz, J. M.; Sambhara, S. TLR7 recognition is dispensable for influenza virus a infection but important for the induction of hemagglutinin-specific antibodies in response to the 2009 pandemic split vaccine in mice. *J. Virol.* **2012**, *86* (20), 10988−10998.
(34) Lowenthal, J. W.; Digby, M. R.; York, J. J. Production of interferon-$\gamma$ by chicken T cells. *Journal of Interferon & Cytokine Research.* **1995**, *15* (11), 933−938.
(35) Tanveer, S.; Malik, H. A.; Shahid, N.; Salisu, I. B.; Ahmed, N.; Latif, A.; Yasmeen, A.; Hassan, S.; Bakhsh, A.; Rao, A. Q. Production of proinflammatory cytokines by expressing Newcastle disease vaccine candidates in corn. *Journal of King Saud University - Science.* **2023**, *35* (3), No. 102537.
(36) Olejniczak, K.; Kasprzak, A. Biological properties of interleukin 2 and its role in pathogenesis of selected diseases–a review. *Med. Sci. Monit.* **2008**, *14* (10), RA179−RA189.
(37) Kak, G.; Raza, M.; Tiwari, B. K. Interferon-gamma (IFN-$\gamma$): Exploring its implications in infectious diseases. *Biomol Concepts.* **2018**, *9* (1), 64−79.
(38) Pishesha, N.; Harmand, T. J.; Ploegh, H. L. A guide to antigen processing and presentation. *Nat. Rev. Immunol.* **2022**, *22* (12), 751−764.
(39) Hall, T. *Nucleic acids symposium series*. Information Retrieval Ltd, 1999, 95−98.
(40) Thompson, J. D.; Higgins, D. G.; Gibson, T. J. CLUSTAL W: improving the sensitivity of progressive multiple sequence alignment through sequence weighting, position-specific gap penalties and weight matrix choice. *Nucleic Acids Res.* **1994**, *22* (22), 4673−80.
(41) de Almeida, R. S.; Maminiaina, O. F.; Gil, P.; Hammoumi, S.; Molia, S.; Chevalier, V.; Koko, M.; Andriamanivo, H. R.; Traoré, A.; Samaké, K.; Diarra, A.; Grillet, C.; Martinez, D.; Albina, E. Africa, a reservoir of new virulent strains of Newcastle disease virus? *Vaccine* **2009**, *27* (24), 3127−3129.
(42) Fatoba, A. J.; Adeleke, V. T.; Maharaj, L.; Okpeku, M.; Adeniyi, A. A.; Adeleke, M. A. Design of a multiepitope vaccine against chicken Anemia virus disease. *Viruses.* **2022**, *14* (7), 1456.
(43) Wilkins, M. R.; Gasteiger, E.; Bairoch, A.; Sanchez, J. C.; Williams, K. L.; Appel, R. D.; Hochstrasser, D. F.; Link, A. J. Protein identification and analysis tools in the ExPASy server. *Methods Mol. Biol.* **1998**, *112*, 531−552.


https://doi.org/10.1021/acsomega.4c09890
*ACS Omega* 2025, 10, 4007−4018

(44) Hebditch, M.; Carballo-Amador, M. A.; Charonis, S.; Curtis, R.; Warwicker, J. Protein−Sol: a web tool for predicting protein solubility from sequence. *Bioinformatics.* **2017**, *33* (19), 3098−3100.
(45) Doytchinova, I. A.; Flower, D. R. VaxiJen: a server for prediction of protective antigens, tumour antigens and subunit vaccines. *BMC Bioinf.* **2007**, *8* (1), 4−4.
(46) Dimitrov, I.; Bangov, I.; Flower, D. R.; Doytchinova, I. AllerTOP v.2—a server for in silico prediction of allergens. *J. Mol. Model.* **2014**, *20* (6), 2278.
(47) Ko, J.; Park, H.; Heo, L.; Seok, C. GalaxyWEB server for protein structure prediction and refinement. *Nucleic Acids Res.* **2012**, *40* (W1), W294−W297.
(48) Jumper, J.; Evans, R.; Pritzel, A.; Green, T.; Figurnov, M.; Ronneberger, O.; Tunyasuvunakool, K.; Bates, R.; Žídek, A.; Potapenko, A.; Bridgland, A.; Meyer, C.; Kohl, S. A. A.; Ballard, A. J.; Cowie, A.; Romera-Paredes, B.; Nikolov, S.; Jain, R.; Adler, J.; Back, T.; Petersen, S.; Reiman, D.; Clancy, E.; Zielinski, M.; Steinegger, M.; Pacholska, M.; Berghammer, T.; Bodenstein, S.; Silver, D.; Vinyals, O.; Senior, A. W.; Kavukcuoglu, K.; Kohli, P.; Hassabis, D. Highly accurate protein structure prediction with AlphaFold. *Nature.* **2021**, *596* (7873), 583−589.
(49) Heo, L.; Park, H.; Seok, C. GalaxyRefine: protein structure refinement driven by side-chain repacking. *Nucleic Acids Res.* **2013**, *41* (W1), W384−W388.
(50) Wiederstein, M.; Sippl, M. J. ProSA-web: interactive web service for the recognition of errors in three-dimensional structures of proteins. *Nucleic Acids Res.* **2007**, *35* (suppl_2), W407−W410.
(51) Laskowski, R.; Macarthur, M. W.; Moss, D. S.; Thornton, J. PROCHECK: A program to check the stereochemical quality of protein structures. *J. Appl. Crystallogr.* **1993**, *26*, 283−291.
(52) Biovia Dassault Systèmes *Discovery Studio Visualizer*. Dassault Systèmes: San Diego, 2017.
(53) Zardecki, C.; Dutta, S.; Goodsell, D. S.; Voigt, M.; Burley, S. K. RCSB Protein Data Bank: A resource for chemical, biochemical, and structural explorations of large and small biomolecules. *J. Chem. Educ.* **2016**, *93* (3), 569−575.
(54) Kozakov, D.; Hall, D. R.; Xia, B.; Porter, K. A.; Padhorny, D.; Yueh, C.; Beglov, D.; Vajda, S. The ClusPro web server for protein−protein docking. *Nat. Protoc.* **2017**, *12* (2), 255−278.
(55) Abramson, J.; Adler, J.; Dunger, J.; Evans, R.; Green, T.; Pritzel, A.; Ronneberger, O.; Willmore, L.; Ballard, A. J.; Bambrick, J.; Bodenstein, S. W.; Evans, D. A.; Hung, C.-C.; O'Neill, M.; Reiman, D.; Tunyasuvunakool, K.; Wu, Z.; Žemgulytė, A.; Arvaniti, E.; Beattie, C.; Bertolli, O.; Bridgland, A.; Cherepanov, A.; Congreve, M.; Cowen-Rivers, A. I.; Cowie, A.; Figurnov, M.; Fuchs, F. B.; Gladman, H.; Jain, R.; Khan, Y. A.; Low, C.M. R.; Perlin, K.; Potapenko, A.; Savy, P.; Singh, S.; Stecula, A.; Thillaisundaram, A.; Tong, C.; Yakneen, S.; Zhong, E. D.; Zielinski, M.; Žídek, A.; Bapst, V.; Kohli, P.; Jaderberg, M.; Hassabis, D.; Jumper, J. M. Accurate structure prediction of biomolecular interactions with AlphaFold 3. *Nature.* **2024**, *630* (8016), 493−500.
(56) Xue, L. C.; Rodrigues, J. P.; Kastritis, P. L.; Bonvin, A. M.; Vangone, A. PRODIGY: a web server for predicting the binding affinity of protein−protein complexes. *Bioinformatics.* **2016**, *32* (23), 3676−3678.
(57) Laskowski, R. A.; Jabłońska, J.; Pravda, L.; Vařeková, R. S.; Thornton, J. M. PDBsum: Structural summaries of PDB entries. *Protein Sci.* **2018**, *27* (1), 129−134.
(58) Lopéz-Blanco, J. R.; Garzón, J. I.; Chacón, P. iMod: multipurpose normal mode analysis in internal coordinates. *Bioinformatics.* **2011**, *27* (20), 2843−2850.
(59) Rapin, N.; Lund, O.; Bernaschi, M.; Castiglione, F. Computational Immunology Meets Bioinformatics: The use of prediction tools for molecular binding in the simulation of the immune system. *PLoS One.* **2010**, *5* (4), No. e9862.
(60) Allan, W. H.; Lancaster, J. E.; Toth, B. *Vaccin contre la maladie de Newcastle*. FAO Animal Production: Rome, 1978; p 176.


https://doi.org/10.1021/acsomega.4c09890
*ACS Omega* 2025, 10, 4007−4018